Break-up of nano-particle agglomerates by hydrodynamically limited processes

Break-up of nano-particle agglomerates by hydrodynamically limited processes

L. Xie [a], C. D. Rielly [a] and G. Özcan-Taşkin [b]*

[a] Department of Chemical Engineering, Loughborough University, Loughborough, Leics., LE11 3TU, UK; email: C.D.Rielly@lboro.ac.uk

[b] BHR Group Ltd, Cranfield, Bedfordshire, MK43 0AJ, UK

ABSTRACT

When dry nano-particulate powders are first added into a liquid, clusters as large as hundreds of microns can be formed. In this study, high shear impellers, such as the sawtooth Ekatomizer and rotor-stator impellers were used to suspend and break-up these agglomerates in a stirred vessel. The high local energy dissipation rates generated by these impeller could slowly break up clusters to sub-micron sizes by an erosional mechanism. In comparison, single and multiple passes through a valve homogeniser could quickly break the nano-particle clusters to sub-micron sizes; single pass operation had the highest breakage efficiency for a given specific energy input. For both equipment types, the rate of fines generation was found to be controlled by the maximum energy dissipation rate. However, the size of the fine aggregates produced was a constant and was not a function of the energy dissipation rate.

1 INTRODUCTION

Dispersion of nano-particle powders into a liquid typically involves three parallel processing operations: (i) wetting and incorporation of the dry powders, which often form large agglomerates; (ii) de-agglomeration to meet the product specifications in terms of the particle size distribution and (iii) stabilization using surfactants and thickeners and thereby the formation of a stable micro-structure. The study described here is part of an EC funded project, PROFORM, which examines a number of different chemical, hydrodynamic and mechanical mechanisms and a range of equipment, for processing of nano-particles into formulated products dispersed in a liquid phase. In practice, although the primary particle size may be of O(10) nm, the larger agglomerates formed are within the inertial sub-range, O(1-100) μm and thus hydrodynamic forces can be effective at breaking these clusters. To create sub-micron sizes requires a combination of chemical effects to destabilise the agglomerates and very high local energy dissipation rates, ε_{max}, which are not normally economic to obtain in stirred tank reactors (STRs). However, the controlled wetting of powders is difficult to achieve in high shear devices, such as in-line rotor-stators or valve homogenizers. Hence the STR is often used to perform wetting and preparation of a crude suspension, which is then fed to more intensive mixers to achieve the final product specifications. Blockage of valve homogenisers can occur if the crude dispersion contains large agglomerates and thus the STR must reduce particle sizes to an acceptable level before more intensive processing takes place. The work described here examined the use of both STRs and valve homogenisers for dispersion.

Hansen *et al*. (1998) define useful terminology for use in connection with the dispersion of solids: powders are said to consist of *agglomerates* which are made up of a collection of *aggregates*. The agglomerates can be broken down by the flow, whereas

the aggregates, which are composed of tightly bound crystals or *primary particles*, cannot be broken by the flow. Hansen & Ottino (1996) and Hansen *et al*. (1998) note that *erosion* is an important mechanism in solids dispersion, in which small aggregates are sheared off from a larger agglomerate. Such a mechanism results in a bi-modal particle size distribution (PSD) of fine and coarse materials.

The flows generated by industrial scale equipment with low viscosity liquids are generally turbulent and so unsteady hydrodynamic stress fluctuations act upon the nano-particle agglomerates. These hydrodynamics stresses may be inertial (Hinze, 1955) or viscous (Baldyga and Bourne, 1994), depending on the size of the agglomerates relative to the Kolmogorov scale, $\lambda_k = (\nu^3/\varepsilon_{max})^{1/4}$. In either case the magnitude of the stress can be expected to depend on the maximum local energy dissipation rate, ε_{max}. If the forces causing deformation exceed the cohesive forces due to inter-particle bonding, then the agglomerate will break-up into smaller fragments. However, compared to liquid-liquid dispersion processes, solid-liquid erosion is much less well understood, because of the problems in establishing the cohesive forces binding together agglomerates, the complexity of the multi-body interactions between aggregates and the effects of irregular agglomerate structures and shapes (Hansen and Ottino, 1998)

In this work, a model system of nano-particulate Aerosil® 200V (fumed silica) in deionised water, without stabilisers was prepared. Fumed silicas are manufactured by flame hydrolysis; although their primary particles have a size of 5–50 nm (depending on the manufacturing conditions) they tend to form stable aggregates of size 100–500 nm, through a combination of hydrogen bonding and sinter bridges formed during the high temperature synthesis process (Gun'ko *et al*., 2001; Degussa, 2006a). Degussa (2006b) state that isolated primary nano-particles do not exist in solution and the aggregates cannot normally be broken by dispersion in a liquid. These aggregates form into loosely

bound and relatively unstable agglomerates, with sizes > 1 μm, which are held together by hydrogen bonds, and electrostatic and polar interactions (Gun'ko *et al.*, 2001).

The de-agglomeration performance of various types of impellers, which generate different pumping capacities, flow patterns and specific power inputs have been studied previously by Xie *et al.* (2006). Low ε_{max} devices were found to be unable to generate sub-micron agglomerates. In the current contribution, results from two high ε_{max} devices, operated within a STR, are compared with data obtained from a valve homogeniser. The de-agglomeration process was then characterized using estimates of the local energy dissipation rate.

2 EXPERIMENTAL

2.1 Experimental set-up

The experimental data reported here were obtained using a model nano-particle system, Aerosil® 200V (Degussa) which is a densified hydrophilic fumed silica (> 99.8% SiO_2 by weight). The solid nano-powder has a specific surface area of 200 m^2/g. The primary particle has an average size ~12 nm and its tapped density is approximately 120 kg/m^3. The liquid used was de-ionised water, which had an electrical conductivity less than 1 μS cm^{-1}. Zeta potential measurements (not shown) indicated that the stability of Aerosil agglomerates is approximately the same for ultra-pure, deionised and distilled water. When Aerosil is added to de-ionised water, the solution pH falls to about 4, which is slightly above the iso-electric point of between pH 1.8 – 3.5. Under these acidic conditions, silica hydrosols are known to be surprisingly stable (Despasse, 1997). Preliminary experiments showed that the size of agglomerates formed did not depend on the quality of the water used. Moreover, the dispersions formed were stable and re-agglomeration did not occur during storage over periods of several days.

The de-agglomeration experiments were performed in a 305 mm diameter cylindrical tank with a torispherical base, as shown in Figure 1. Four equally spaced baffles were mounted on the walls of the tank. In the experiments discussed here the mass fraction of solids was 1%, although higher concentrations were also studied.

Özcan-Taskin *et al.* (2006) showed that the time required for wetting and draw-down of initially dry Aerosil 200V powders, added to the surface of a stirred vessel, depends on the solids mass fraction, the impeller type, position and the rotational speed. In such a situation, the initial agglomerates enter the flow at different times and with a broad range of sizes. To avoid inconsistencies with the dynamics of the initial wetting stage, a procedure was developed to add hand-mixed wetted Aerosil® 200V into the liquid in the STR at the 1 % mass concentration. The crude dispersion produced by hand-mixing was shown to have a very reproducible size distribution and thus provided a consistent starting point for the de-agglomeration studies.

2.2 Equipment investigated in the de-agglomeration experiments

The geometric details and dimensions of the Ekatomizer impeller used in the experiments are presented in Table 1 and Figure 2. The EkatoMizer is a sawtooth impeller which is able to generate a high local energy dissipation rate (Beck, 1998), but only a weak discharge flow. The EkatoMizer was either used individually or was combined with other axial/radial flow impellers which ran from a different central shaft (details of these impellers are in Table 1). A series of de-agglomeration experiments were carried out using a variety of impeller configurations and rotational speeds covering a range of mean specific power inputs up to 3 kW/m^3 and a range of estimated ε_{max} values up to about 0.3 kW/kg. (The method for estimating ε_{max} is discussed in §3.4.) In addition, two sizes of IKA Ultra-Turrax® rotor-stators (not geometrically similar)

were used to provide high ε_{max} values with tank average values up to 6 kW/m^3 and ε_{max} up to about 9 kW/kg.

An APV Gaulin 15MR high pressure valve homogeniser was also used in the de-agglomeration experiments. The homogenisation flow rate was 990 mL/min for all experiments. The valve seat was a ceramic cell disruption (CD) type, with an 11.0 mm impact ring. The homogenisation pressure was varied from 400 to 8000 psi (27 – 550 bar). The homogeniser and its valve parts are illustrated in Figure 3 and Figure 4.

2.3 Sampling and data analysis

Samples of the dispersion were withdrawn, at specific times from the stirred tank using a wide bore pipette, to follow the dynamics of the PSD evolution. Samples were taken from the product tube (3 in Figure 3) of the valve homogeniser. The samples were analysed by laser diffraction, using a Malvern Mastersizer® S, to yield the PSD which was expressed as a *volume* probability density function, q_3. A 'polydisperse' analysis model was chosen in the calculation of the PSD and a complex refractive index $1.46 + 0.1i$ was applied in all data analysis presentations. Further details of the measurement technique were presented by Xie *et al.* (2006).

3 RESULTS AND DISCUSSION

3.1 Higher energy dissipation impellers: EkatoMizer and rotor-stators

The EkatoMizer saw-tooth impeller is designed to be operated at very high rotational speeds (typically thousands of rpm) for operations such as liquid-liquid dispersion or fine powder de-agglomeration. At these high speeds the EkatoMizer will produce higher local ε_{max}, values (estimates were obtained using the approximate

method described in §3.4; the ratio of $\varepsilon_{max}/\bar{\varepsilon}$ is estimated to be O(10^2) for the EkatoMizer; Beck (1998) obtained $\varepsilon_{max}/\bar{\varepsilon} = 30$ using LDA measurements.

Figures 5 and 6 show that for the EkatoMizer, the mean particle sizes continued to decrease for one hour and had not reached a steady or equilibrium PSD. The development of a second mode in the sub-micron range of the PSD in Figure 5, after about 15-30 minutes, indicates that this impeller is capable of generating finely dispersed aggregates. In contrast, no sub-micron fines were generated using the LE-20, PBT and 6DT impellers alone (Xie *et al.*, 2006).

Figure 6 presents the evolution of the agglomerate $D[3,2]$ at four EkatoMizer speeds, all starting from the same hand pre-mixed dispersion ($D[3,2] \approx 60$ μm). At the lowest speed of 750 rpm, the agglomerate mean sizes are 30–40 μm, which is comparable to the dispersions produced by the low ε_{max} single impellers (LE-20, PBT and 6DT studied by Xie *et al*. (2006)). At the higher EkatoMizer speeds, these large agglomerates were slowly broken up and the PSD moved to the left, as shown in Figure 5. Above 2200 rpm, a second mode appeared in the PSD, indicating that sub-micron particles have been produced by the high local energy dissipations rates generated by the EkatoMizer. The rate at which these fines were generated is very slow compared to a typical blending time for the STR and would have continued beyond the duration of the experiment. This low rate of particle breakage may be attributed to (i) the intermittent nature of the energy dissipation (see Pope (2000) for a full discussion of internal intermittency); (ii) the low volume fraction of the regions containing high dissipation rates and (iii) the frequency at which agglomerates are circulated back to the impeller.

When one of the high speed rotor-stators (see Figure 7) was used in the stirred tank, the agglomerates were broken up more rapidly, due to the higher ε_{max} of these

devices. A second mode of sub-micron fines appeared in the PSD after about 1-5 minutes (see Figure 8). Compared with the EkatoMizer at similar times and mean power inputs (comparable energy densities, E_v), the volume fractions contained in the fine particle modes of the PSDs generated by the rotor-stator were larger, *i.e.* the breakage rates were much greater. In Figure 9 the agglomerate mean size $D[3,2]$ decreases quickly from its initial value of about 60 μm and falls to less than 2 μm after 60 min; the average agglomerate sizes are sub-micron after three hours of agitation. As shown in Figure 6 and Figure 9, the mean P/V for the T25 rotor-stator is greater than for the EkatoMizer impeller. Moreover, if it is assumed that dissipation predominantly occurs within the swept volume of the rotor-stator, then the Ultra-Turrax T25 and T50 should give much higher *local* ε_{max} values than the EkatoMizer (see §3.4).

3.2 Combination of low and high energy dissipation impellers

Further experiments were carried out using combinations of low and high energy dissipation impellers. Figure 10 presents three experiments run at approximately the same total power input, with different EkatoMizer and dual LE-20s speeds; the speed of the EkatoMizer determines ε_{max} and hence the mean size of the agglomerates. Although the data are not completely consistent, the mean sizes $D[3,2]$ are usually greater for the lower EkatoMizer speeds, even though the total specific power input remains constant. These results support the conclusion that the maximum local energy dissipation rate controls the kinetics of the de-agglomeration process, rather than the mean P/V. Although the PBT helps in generating the bulk flows in the tank, its effect is limited, because the EkatoMizer itself generates sufficient discharge flow for macro-mixing at high rotational speeds.

This finding is confirmed by the results shown in Figure 11, which shows a series of experiments run at a fixed EkatoMizer speed (hence constant ε_{max}) with various

PBT power inputs. Adding a PBT impeller and increasing its power input up to 16.5% of the total energy input, results in no change in D[3,2] produced by the EkatoMizer alone.

Similar results were found with a rotor-stator (T25) and PBT combination, as shown in Figure 12: maintaining a constant ε_{max} (controlled by the T25 speed) showed no change in D[3,2] when the PBT power input was increased.

Conversely, keeping the PBT power input constant and increasing the ε_{max} produced by the T25, resulted in the production of smaller agglomerates. Thus in both cases the high energy dissipation devices, the EkatoMizer or the T25, control the value of ε_{max} and hence determine the kinetics of the de-agglomeration process and the mean sizes, D[3,2], of agglomerates produced (but not the size of the fine aggregates).

3.3 De-agglomeration using a valve homogeniser

De-agglomeration experiments were carried out using the APV homogeniser. Figure 13 shows a series of single pass experiments run at various operating pressure drops across the valve. At very low pressure (400 psi) a sub-micron peak was observed in the PSD curve. As the pressure drop was increased, this peak appeared to increase in volume %, whilst the coarse (right hand) peak of the PSD shifted to smaller sizes. Figure 14 gives the agglomerate PSDs after multiple homogenisation passes for a constant operating pressure drop of 600 psi. As the number of passes increased, more and more sub-micron particles could be found. However, after four passes the sub-micron peak increased slowly, with a third mode appearing above 100 μm after 5 passes, which may be a measurement anomaly. Both the PSD curve evolutions and the range of sub-micron particles produced are qualitatively similar to the high speed rotor-stator results.

3.4 Analysis of the rate of production of fine particles

The formation of bimodal size distributions is typical of an erosional breakage mechanism (Hansen and Ottino, 1996). In most of the experimental PSDs, the lower modes (fine agglomerates) were in the sub-micron scale, whereas the upper modes (coarse agglomerates) were usually above 1 μm. This suggests an erosional mechanism, by which loosely-attached sub-micron aggregates are broken away slowly from larger agglomerates, at a rate determined by the extremes of the intermittent turbulence dissipation rates and the circulation frequency back to the impeller region. With non-overlapping modes, such as shown in Figure 5, 10 and 13-14, it is straightforward to obtain the volume fraction of fine particles in the PSD; here fine particles have been defined to belong to the lower mode, with a maximum cut-off of 1 μm.

Figure 15 shows a comparison of the rate of fines generation by the rotor-stator and APV valve homogeniser, plotted against the specific energy input (the Δp across the valve homogeniser is equivalent to an energy input per unit volume, 1 psi = 6890 Pa = 6.89 kJ/m^3). The power inputs of the impellers over a range of rotational speeds were measured using a well-insulated calorimetric experiment,: the power numbers, *Po*, were constant with values of 3.9 and 1.0 for the T25 and T50 rotor-stators (the rotor diameter has been used to calculate the power number *Po* and the rotor-stators are not geometrically similar).

Wu and Patterson (1989) found that about 30% of the power of the 6DT was dissipated in the impeller region, whereas Zhou & Kresta (1996) estimated this to be about 50% for the PBT. More recently, using particle image velocimetry methods, Khan *et al*. (2006) showed that for a $D = T / 3$ PBT, about 40% of the dissipation occurred inside the swept volume. Thus the proportion of the total power input dissipated in the impeller region depends on the impeller type and D/T ratio. However, a crude, order of

magnitude estimate of the maximum dissipation rate may be obtained assuming that about 40% of the power input is dissipated close to all of the impellers used here, leading to the following equation.

$$\varepsilon_{\max} = \frac{0.4PoN^3D^5}{V_{swept}} \qquad (1)$$

In practice, intermittency and gradients in the dissipation rate within the swept volume, mean that eq.(1) is likely to provide an underestimate of ε_{max}. These estimates of ε_{max} are shown in Figure 15; the corresponding Kolmogorov scales are about 3-7 μm, which are smaller than the largest agglomerate sizes in most cases, indicating that inertia could be still be an effective breakage mechanism.

Comparison of Figure 5, 10, 13 and 14 shows that the size of fine particles produced remained constant at around 300 nm for different deagglomeration times and for different mean specific power inputs. Moreover, estimates based on eq.(1) show that the EkatoMizer and T25 rotor-stator have very different $\varepsilon_{\max}$ values and yet the size of the fines produced were the same. The small swept volume and larger power number gave larger values of ε_{max} for the T25 than the T50. For both rotor-stators, decreasing the rotational speed (and hence ε_{max}) resulted in a decrease in the rate at which fines are generated. Operation at 11 000 rpm with the T25 and 7500 rpm with the T50 rotor-stator gave about the same value of $\varepsilon_{\max}$ and similar rates of fines generation (see Figure 15) were obtained, which again tends to confirm that $\varepsilon_{\max}$ controls the kinetics of de-agglomeration. For the valve homogeniser single and multiple passes, increasing the pressure, Δp, or number of passes, n, (the energy density is $E_v = n\Delta p$) resulted in an increase in the rate of fines generated. Figure 15 also shows single pass has much faster fines generating rates than multiple passes at the same specific energy. It is difficult to estimate the local $\varepsilon_{\max}$ in the throat of the valve, because of the uncertainty in the

volume in which the dissipation takes place. However, at a given E_v, a single pass operation has much larger ε_{max} than for a multiple pass operation and hence more efficient breakage of agglomerates is obtained. In Figure 15 a single pass at 4000 psi, results in a greater volume of fines being produced, than 10 passes at 400 psi. Furthermore from Figure 15 it can be concluded for a given energy density, E_v, compared to rotor-stators, the valve homogeniser has a much higher breakage efficiency, which increases with the local value of ε_{max} in the throat of the valve.

For all operating conditions, *i.e.* covering a wide range of specific power inputs and ε_{max} values, the mean size, $D[3,2]$, of the fine particle mode alone, remained constant at about 300 nm. Therefore, the slow change of $D[3,2]$ for the whole PSD, shown for example in Figure 11, is due to erosion of large agglomerates to form an increasing volume fraction of fine aggregates of around 300 nm in size.

Equation (1) may also be used to estimate ε_{max} values for the other impellers. For example, at 2200 rpm with the EkatoMizer (the lowest speed at which sub-micron fines were generated), eq.(2) yields that $\varepsilon_{max} \approx 0.2$ kW/kg . In that case, fines were extremely slowly produced and were not detected until after 60 min, which is broadly consistent with the rotor-stator results of Figure 15.

4 CONCLUSIONS

At low impeller speeds, the EkatoMizer impeller did not provide much breakage of the agglomerates, due to the small values of ε_{max} generated. Almost all the size reduction occurred in the first few minutes of operation. At higher speeds, the EkatoMizer generated a higher ε_{max} and the Aerosil agglomerates were broken into sub-micron aggregates with a constant size of about 300 nm size. A study of various impeller combinations showed that the kinetic rate of the de-agglomeration process was

controlled by the value of ε_{max} produced by the high shear devices and was unaffected by any additional power input from the LE-20 or PBT impellers.

The most successful STR dispersion devices were the rotor-stators, which were able to generate very high ε_{max} values and hence sub-micron aggregates. Order of magnitude type estimates of ε_{max} values were obtained by assuming that a fixed fraction of the power was dissipated within the impeller volume. Using these estimates it was possible to show that the rate at which fines were generated depended on the maximum dissipation rate. The largest agglomerate sizes produced were in the inertial subrange, but the smallest were sub-Kolmogorov in size and hence it is likely that a combination of inertial and viscous shear mechanisms are responsible for breakage.

The valve homogeniser also proved to be a successful dispersion device, because of the very high local energy dissipation rates generated in the valve gap. Single pass experiments with a large Δp were more effective at generating fines than multiple passes with a lower Δp, confirming that for a fixed value of the energy density, the rate of generation of fine aggregates increased with increasing ε_{max}.

The experimental finding that the PSD develops into a bi-modal distribution for the high ε_{max} impellers indicates that the Aerosil® 200V agglomerates are broken up by an erosional process, in which fine aggregates are slowly removed by hydrodynamic shear stresses from the main agglomerate. Thus there is no equivalent of the equilibrium PSD from the Kolmogorov-Hinze theories of droplet breakage and the size of the fine aggregates produced has been found to be independent of processing time, ε_{max} and the mean specific power input. Their sizes are around 300 nm, which is in the range of 100-500 nm quoted by Gun'ko *et al.* (2001) for the closely bound aggregates of primary silica particles. In STRs, the de-agglomeration process happens rather slowly, probably due to the intermittent nature of the extreme turbulence kinetic energy dissipation

events. In the systems studied here, the $D[3,2]$ of the fine particles is around 300 nm, which is rather far from the manufacturer's claimed primary particle size of 12 nm. So, these fine agglomerates contain $O(10^4)$ primary particles, which are strongly bound to each other and cannot be disrupted by hydrodynamic effects; in contrast, the larger agglomerates can be fragmented by shear stress generated by the flow.

ACKNOWLEDGEMENTS

This study was carried out within the project PROFORM ("Transforming Nano-particles into Sustainable Consumer Products Through Advanced Product and Process Formulation" EC Reference NMP4-CT-2004-505645) which was partially funded by the 6th Framework Programme of EC. The contents of this paper reflects only the authors' view. The authors gratefully acknowledge the useful discussions held with other partners of the Consortium: Karlsruhe University, Inst. of Food Process Eng.; Bayer Technology Services GmbH; Unilever UK Central Resources Ltd.; Birmingham University School of Eng.; Warsaw University of Technology, Dept. of Chemical and Process Eng.; Poznan University of Technology, Inst. of Chemical Tech. and Eng.; Rockfield Software Limited; Centre for Continuum Mechanics.

REFERENCES

Bałdyga J. and Bourne J.R., 1994, "Drop breakup in the viscous subrange: a source of possible confusion", *Chem. Eng. Sci.,* **49**: 1077-1078.

Beck K., 1998, "Mechanisms of drop break-up in stirred vessels using a sawtooth impeller". PhD thesis Cranfield University, School of Mechanical Engineering.

Depasse J., 1997, "Letter to the editor: Coagulation of colloidal Silica by Alkaline Cations: Surface Dehydration or Interparticle Bridging?", *J. Colloid and Interface*

Sci., **194:** 260-262.

Degussa, 2006a, Tech. Bull. No. 11, "Fine Particles: Basic Characteristics of AEROSIL®".

Degussa, 2006b, Tech. Info. No. 1279, "Successful Use of AEROSIL® Fumed Silica in Liquid Systems".

V.M. Gun'ko, V.I. Zarko, R. Leboda, E. Chibowski, 2001, "Aqueous suspension of fumed oxides: particle size distribution and zeta potential", *Adv. in Coll. and Int. Sci.,* **91**, pp.1-112.

Hansen, S. and Ottino, J.M., 1996, "Agglomerate erosion: A nonscaling solution to the fragmentation equation", *Phys. Rev. E* **53**(4): 4209 – 4212.

Hansen, S., Khakhar, D.V. and Ottino, J.M., 1998, "Dispersion of solids in nonhomogeneous viscous flows", *Chem. Eng. Sci.* **53**(10): 1803 – 1817.

Hinze J.O., 1955, "Fundamentals of the hydrodynamics mechanism of splitting in a dispersion process", *A.I.Ch.E. Journal*, **1**: 289-295.

Khan F.R., Rielly C.D. and Brown D.A.R., 2006, "Angle-resolved stereo-PIV measurements close to a down-pumping pitched-blade turbine", *Chem.Eng.Sci*., **61**: 2799 – 2806.

Özcan-Taşkin G., Eagles W., Clements P., Xie L. and Rielly C.D., 2006, "Suspension of fine particles in a liquid using stirred tanks", *12th Eur. Conf. on Mixing* (Bologna, 27-30 June).

Pope, S.B., 2000, "Turbulent Flows", *Cambridge University Press*, Cambridge, UK: 258-259.

Wu H. and Patterson G.K., 1989, “Laser-Doppler Measurements of turbulent flow parameters in a stirred mixer”, *Chem. Eng. Sci*., **44**: 2207-2221.

Xie L., Rielly, C.D., Eagles, W. and Özcan-Taşkin G., , 2006, “De-agglomeration of pre-wetted nano-particles using mixed flow and high shear impellers”, *12th Eur. Conf. on Mixing* (Bologna, 27-30 June).

Zhou G. and Kresta S.M., 1996, “Distribution of energy between convective and turbulent flow for three frequently used impellers”, *Trans IChemE,* **74**A: 379-389.

Table 1. The impeller specification and power number for *C*/*T*=1/3 and *T*=0.305 m

Impeller	Description	*D* [m]	*L* [m]	*W* [m]	*t* [m]	*Po*
LE-20	Hydrofoil impeller (down pumping)	0.152	–	–	–	0.28
PBT	45° pitched 4-bladed turbines	0.150	0.061	0.030	0.0021	1.39
6DT	6-bladed radial disc turbine	0.152	0.038	0.031	0.0017	5.02
EkatoMizer®	Saw-tooth impeller	0.095	–	0.025	0.0030	0.095

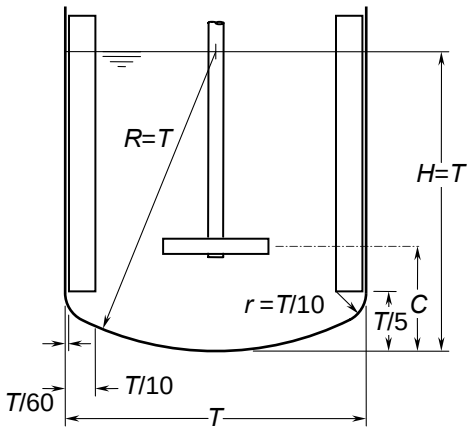

Figure 1. The mixing tank geometry (*T* = 305 mm) used in this study

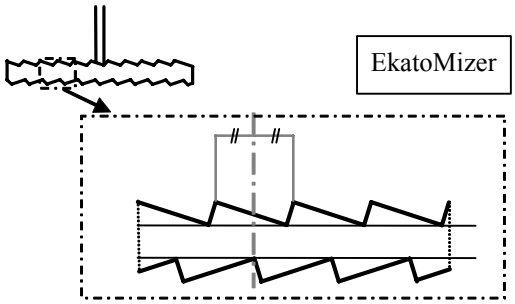

Figure 2. EkatoMizer impeller used in the de-agglomeration experiments.

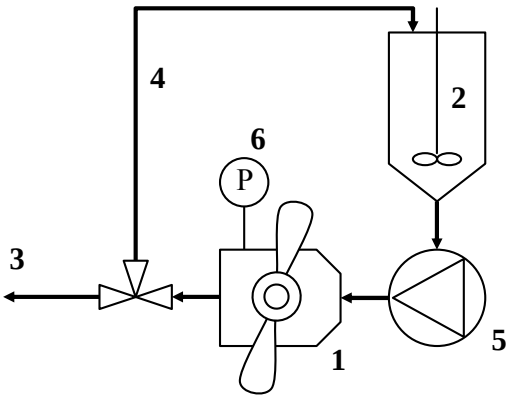

Figure 3. APV Gaulin 15MR homogeniser

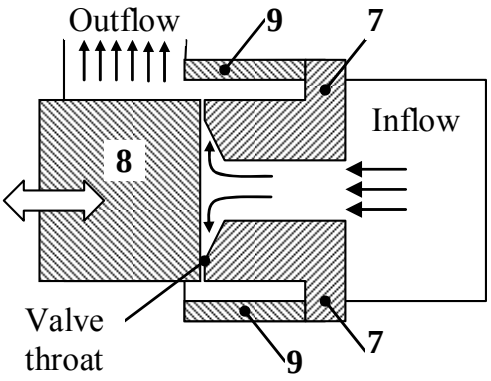

Figure 4. Sketch of the homogeniser valve

1. homogeniser valve body; 2. reservoir tank; 3. product tube; 4. circulation tube; 5. oil pump; 6. pressure gauge; 7. valve seat; 8. valve rod; 9. impact ring.

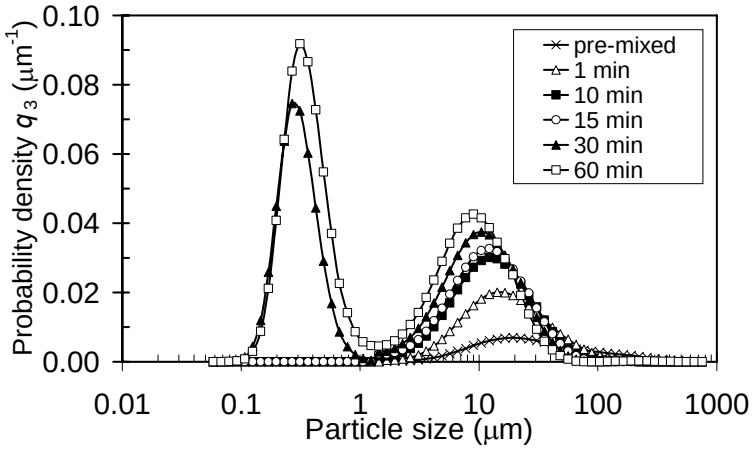

Figure 5. Agglomerate size probability density function for different de-agglomeration times: EkatoMizer impeller at 2600 rpm and *C*=*T*/3. Fines (left peak) can be found after 15 – 30 mins.

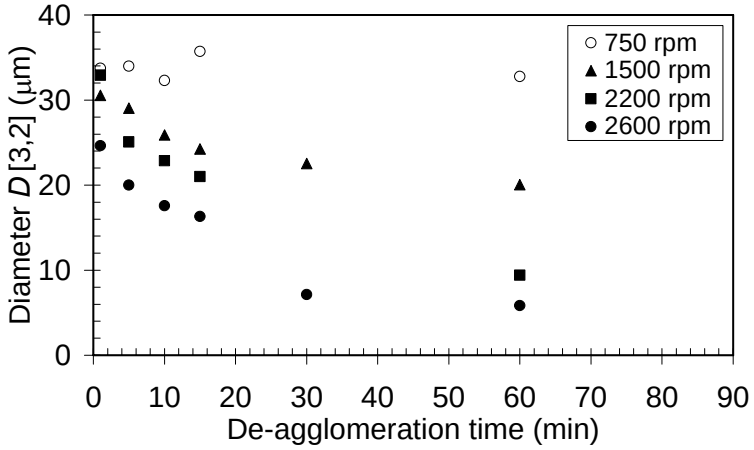

Figure 6. Agglomerate sizes *D*[3,2] *vs.* de-agglomeration time at EkatoMizer speeds of 750, 1500, 2200 and 2600 rpm corresponding to mean *P*/*V* of 0.072, 0.574, 1.812 and 2.991 kW/m^3 respectively.

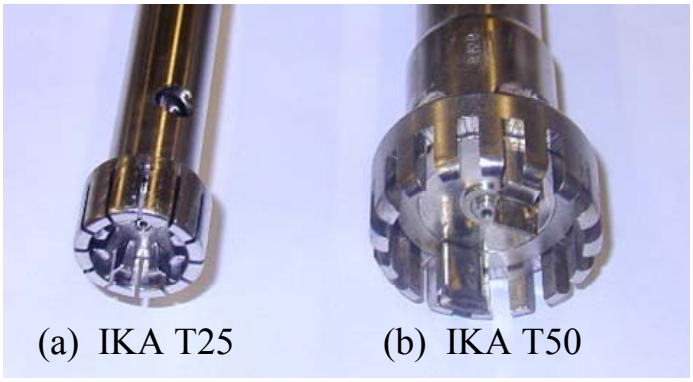

Figure 7. Ultra-Turrax rotor-stator dispersion tool mounted at *C*/ *T* = 1/2 (a) IKA T25 and (b) IKA T50; the outer diameters of the rotor and stator and gap width are respectively (a) 18, 25 and 0.5 mm and (b) 36, 45 and 1 mm.

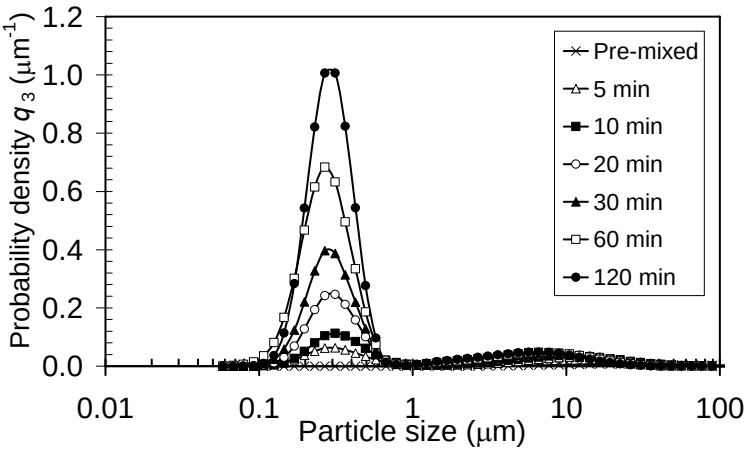

Figure 8. Agglomerate size volume probability density function for different de-agglomeration times: T25 rotor-stator at 16 000 rpm and *C*=*T*/2.

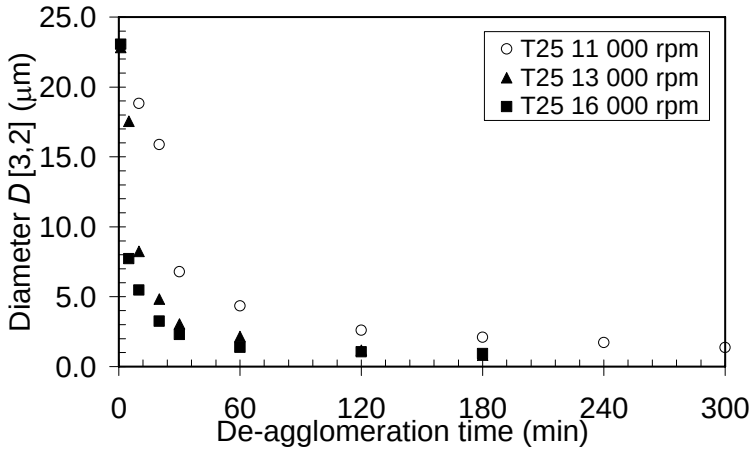

Figure 9. Agglomerate sizes *D*[3,2] *vs.* de-agglomeration time at three T25 rotor-stator speeds of 11 000, 13 000 and 16 000 rpm corresponding to mean *P*/*V* of 2.21, 3.17 and 6.01 kW/m^3, respectively.

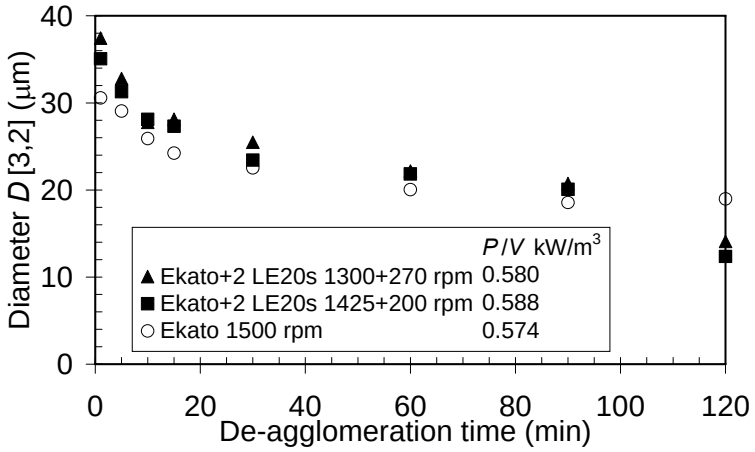

Figure 10. Single EkatoMizer combined with two LE-20 impellers. The EkatoMizer speed was changed from 1300 rpm to 1500 rpm. The total power input in all three experiments was approximately constant.

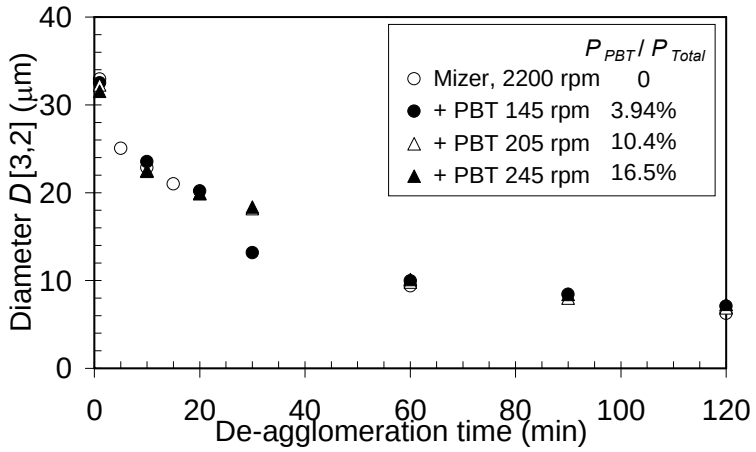

Figure 11. De-agglomeration experiment using a single EkatoMizer in combination with a PBT. The EkatoMizer power input was fixed, whereas the PBT speed was varied from 145 to 245 rpm, changing its power input.

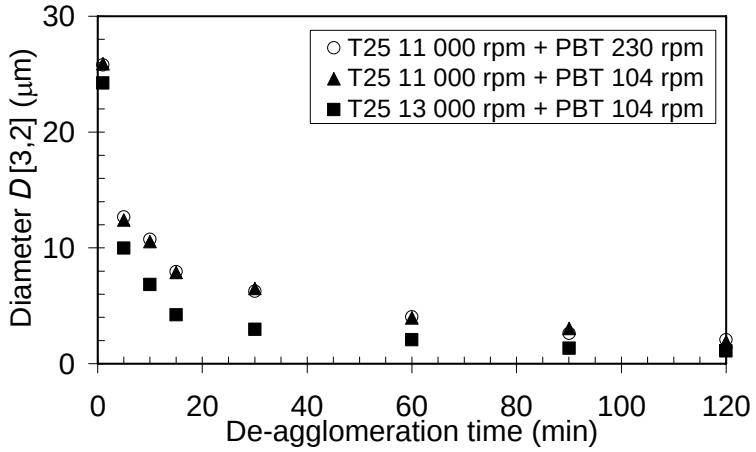

Figure 12. Deagglomeration using a T25 rotor-stator plus a single PBT at three speed combinations.

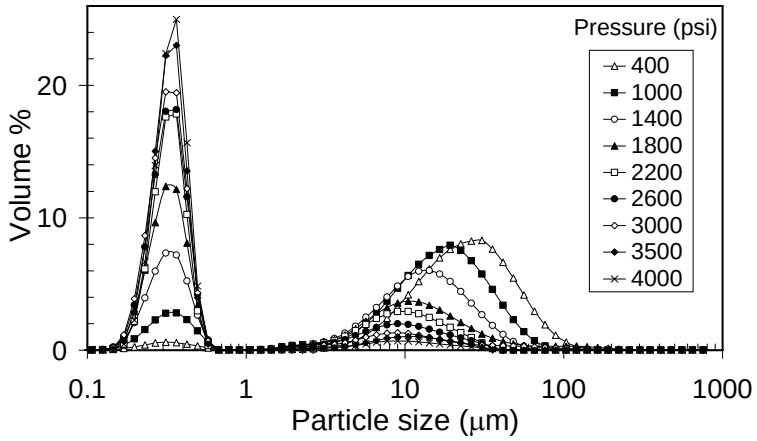

Figure 13. De-agglomeration experiment using an APV homogeniser by single pass configuration (5 % mass solids).

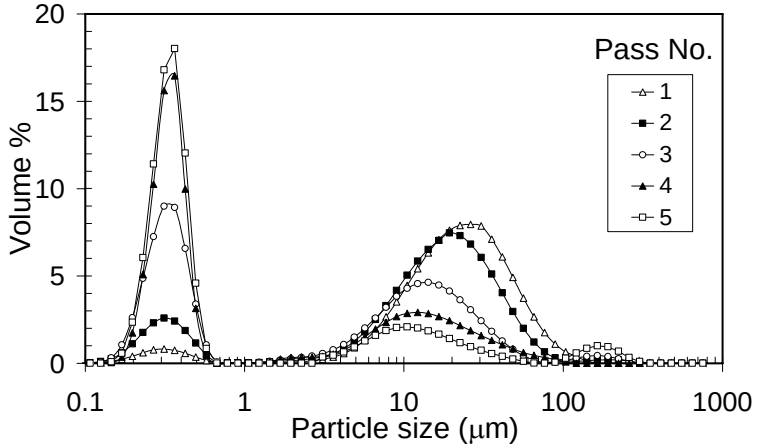

Figure 14. De-agglomeration experiment using an APV homogeniser by multiple passes (5 % mass solids, Δp = 600 psi).

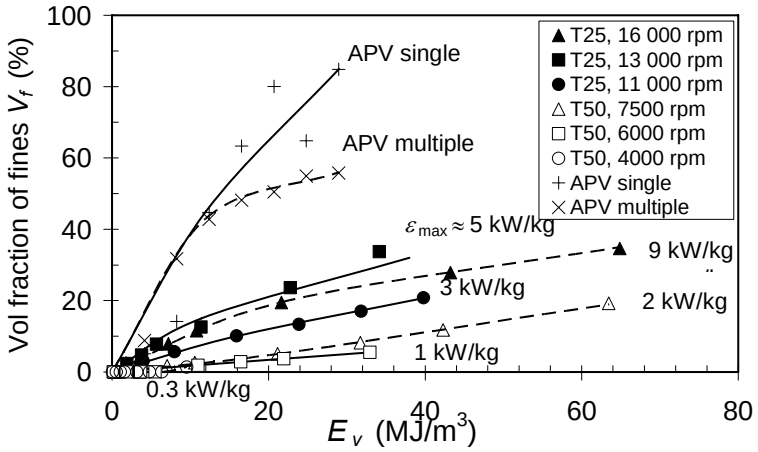

Figure 15. The rate of generation of fines by re-analysis of PSD curves. Estimates of the ε_{max} from eq.(1) for each rotor-stator operation are also shown.